

MyD88 knockout mice develop initial enlarged periapical lesions with increased numbers of neutrophils

R. A. Bezerra da Silva, P. Nelson-Filho, M. P. Lucisano, A. De Rossi, A. M. de Queiroz & L. A. Bezerra da Silva

Department of Pediatric Dentistry, School of Dentistry of Ribeirão Preto, University of São Paulo, Ribeirão Preto, SP, Brazil

Abstract

Bezerra da Silva RA, Nelson-Filho P, Lucisano MP, De Rossi A, de Queiroz AM, Bezerra da Silva LA.

MyD88 knockout mice develop initial enlarged periapical lesions with increased numbers of neutrophils. *International Endodontic Journal*, 47, 675–686, 2014.

Aim To characterize the formation and progression of experimentally induced periapical lesions in teeth of MyD88 knockout (MyD88 KO) mice compared with wild-type (WT) mice.

Methodology Periapical lesions were induced in the mandibular first molars of 30 WT and 30 MyD88 KO mice. After 7, 21 and 42 days, the animals were euthanized and the mandibles were subjected to histotechnical processing. Histological sections were stained with haematoxylin and eosin (HE), TRAP histochemistry, Brown and Brenn staining and immunohistochemistry (RANK, RANKL, OPG). Data were subjected to statistical analysis by the nonparametric Mann–Whitney and Kruskal–Wallis tests and the

Dunn post-test, using the SPSS software, version 17.0 ($\alpha = 0.05$).

Results Regarding the periapical lesion size, the MyD88 KO group had significantly higher values than the WT group in the periods of 7 ($P = 0.001$) and 21 days ($P = 0.05$). A larger number of neutrophils in the MyD88 KO group were observed ($P = 0.01$ at 7 days, $P = 0.004$ at 21 days and $P < 0.001$ at 42 days). Regarding the number of osteoclasts, no statistically significant difference was observed between the groups at any of the experimental periods ($P = 0.884$ at 7 days, $P = 0.506$ at 21 days and $P = 0.211$ at 42 days).

Conclusions In the absence of MyD88, the animals had larger periapical lesions, with a severe inflammatory infiltrate and a significantly larger number of neutrophils.

Keywords: knockout mice, MyD88 molecule, periapical lesion, Toll-like receptors.

Received 3 July 2013; accepted 10 October 2013

Introduction

The activation of the host immunoinflammatory response to infection occurs via pattern recognition receptors (PRRs), which are expressed in different cell compartments and which recognize intracellular and extracellular pathogens. PRRs identify

pathogen-associated molecular patterns (PAMPs), which are structurally conserved antigenic moieties that are found both within the pathogens' surface and structure (Hedayat *et al.* 2012). Toll-like receptors (TLRs) stand out amongst PRRs (Hirao *et al.* 2009, Kawai & Akira 2009), participating in the early recognition of various pathogens and immune response activation (Hedayat *et al.* 2012).

Intracellular pathways of TLRs are activated through Toll/IL-1 receptor (TIR) domain interactions with proteins or adapter molecules that are recruited to the site, amongst which myeloid differentiation factor 88 (MyD88) stands out (Loures *et al.* 2011).

View the pubcast on this paper at

<http://www.scivee.tv/journalnode/62892>

Correspondence: Marília Pacifico Lucisano, Departamento de Clínica Infantil, Faculdade de Odontologia de Ribeirão Preto, USP, Av. do Café, s/n, Monte Alegre, 14040-904 Ribeirão Preto, SP, Brazil (e-mail: marilia.lucisano@usp.br).

MyD88 participates in the activation of all of the TLRs (except TLR3) and triggers the activation of protein kinases and transcription factors that stimulate the expression of genes that are involved in the inflammatory response (Gomes *et al.* 2012). Studies have evaluated the effect of MyD88-dependent signaling in immune system activation and performance in response to infection with different pathogens (Hughes *et al.* 2005, LaRosa *et al.* 2008, Koh *et al.* 2010, Loures *et al.* 2011, Hanke *et al.* 2012, Ishibashi *et al.* 2012). Although the precise contribution of this molecule is not entirely understood, the results tend to indicate that MyD88 plays a key role in controlling infection, the immediate activation of the innate immune system, cytokine production and adaptive immune response activation in late stages (Koh *et al.* 2010).

Toll-like receptors are highly expressed in multiple cell types that are associated with endodontic infections. The activation of these receptors causes the stimulation of multiple pro-inflammatory cytokines, including IL-1, TNF- α and IL-6. These cytokines are involved in the increased production of receptor activator of nuclear factor-kappa B ligand (RANKL), which regulates osteoclastogenesis and bone resorption (Bar-Shavit 2008, Hirao *et al.* 2009).

A recent study evaluated the formation and progress of experimentally induced periapical lesions in TLR2 knockout mice (Da Silva *et al.* 2012). The lack of this receptor was shown to cause the formation of more extensive periapical lesions, with a higher number of osteoclasts than was observed in wild-type (WT) mice. These results indicated a key role of TLR2 during the immunoinflammatory response that is triggered to fight infection of the root canal system and periapical tissue.

Although the role of adapter molecule MyD88 in controlling infection and immune system activation has been examined, its function/involvement in the development and progression of periapical lesions has not been investigated. For these reasons, the aim of the current study was to describe the formation and progression of experimentally induced periapical lesions in the teeth of MyD88 knockout mice compared with WT mice. This analysis was performed with conventional light microscopy, fluorescence microscopy, tartrate-resistant acid phosphatase (TRAP) histochemistry, Brown and Brenn staining and immunohistochemistry. The null hypothesis was that the formation and progression of periapical lesions would not be different between MyD88 knockout and WT mice.

Materials and methods

The current research project was initially submitted and approved by the Ethics Committee on Animal Use of the University of São Paulo (Comissão de Ética no Uso de Animais da Universidade de São Paulo, USP), Ribeirão Preto Campus (Case no. 11.1.91.53.0). Thirty male WT C57BL/6 mice between 6 and 8 weeks of age were used. The mice weighed an average of 20 grams and were purchased from the Central Animal Facility of the University of São Paulo (Biotério Central da Universidade de São Paulo), Ribeirão Preto Campus. Thirty C57BL/6 MyD88 knockout mice (MyD88 KO) were also examined, which were provided by the Genetics Animal Facility of the School of Medicine of Ribeirão Preto (Biotério de Genética da Faculdade de Medicina de Ribeirão Preto), USP and from The Jackson Laboratory, Bar Harbor, ME, USA. All of the animals were maintained in the animal facility of the School of Dentistry of Ribeirão Preto (Faculdade de Odontologia de Ribeirão Preto), USP, and received routine care.

The induction of periapical lesions

The animals were anaesthetized intramuscularly with ketamine (10% ketamine, Agener União Química Farmacêutica Nacional S/A, Embu-Guaçu, São Paulo, Brazil) at a dose of 150 mg kg⁻¹ body weight and 2% xylazine (Dopaser, Laboratórios Calier, SA, Barcelona, Spain) at a dose of 7.5 mg kg⁻¹ body weight to perform the surgical procedures.

The induction of periapical lesions was performed on the mandibular first molars, totalling 60 teeth for each group of animals. Initially, the crown opening was performed via the occlusal surface using a stainless steel round bur (no. ¼ - GDK Densell Dental Technology, Buenos Aires, Argentina) that was mounted on a low-speed handpiece. The root canals were located using a sterilized endodontic number 08 K-file (Dentsply Maillefer, Ballaigues, Switzerland) and were exposed to the oral environment to induce periapical lesions. Following periods of 7, 21 and 42 days, the animals were randomly submitted to euthanasia in a CO₂ chamber.

Histotechnical processing and microscopic evaluation

Following euthanasia, the mandibles were removed, fixed, decalcified and submitted to routine histological processing (Da Silva *et al.* 2012). Semi-serial

5- μm -thick sections were longitudinally cut throughout the length of the periapical lesion.

Sections that were representative of each experimental group were stained with haematoxylin and eosin (H&E) and submitted to light microscopy analysis to observe the features of the root canal and the periapical and apical regions and to count the number of inflammatory cells (neutrophils). A parallel morphometric analysis of the area of the periapical lesions using fluorescence microscopy was performed. Subsequently, sequential specimens were evaluated by (i) TRAP activity histochemistry to identify and count the osteoclasts, (ii) Brown and Brenn staining to identify the presence and location of bacteria and (iii) immunohistochemistry to identify osteoclastogenesis markers (receptor activator of nuclear factor κ B [RANK], RANKL and osteoprotegerin [OPG]).

All of the analyses were performed using an Axio Imager.M1 microscope (Carl Zeiss MicroImaging GmbH, Göttingen, Germany) that was coupled to an AxioCam MRc5 camera (Carl Zeiss MicroImaging GmbH). The analyses were only performed in the distal roots of mandibular first molars using sections simultaneously showing the coronal, the middle and the apical thirds of the root canal, the apical foramen and the alveolar bone. All of the analyses were performed by a single experienced assessor, without prior knowledge of the group under analysis.

Descriptive microscopic analysis of the characteristics of the root canal and the apical and periapical regions

The descriptive analysis of the root canal and the periapical and apical regions was performed on sections that were representative of each period and each experimental group, according to the following parameters (Da Silva *et al.* 2012): root canal: necrosis (total or partial); apical cementum: surface characteristics (regular or irregular); periodontal ligament: size (normal or increased), the characteristics of the inflammatory cell infiltrate and the presence of oedema and collagen fibres; alveolar bone: the absence/presence of resorption, osteoclasts and osteoblasts.

Fluorescence microscopy morphometrics

The morphometric assessment of the area of the periapical lesions was performed on the H&E-stained specimens using an Axio Imager.M1 microscope at 10 \times magnification, operating in fluorescence mode, as

described by De Rossi *et al.* (2007) and Da Silva *et al.* (2012). The size of the periapical lesion was outlined and measured in μm^2 , excluding the intact structures (i.e. the periodontal ligament, the cementum and the alveolar bone), which were easily identified by strong green fluorescence, and including areas of resorption and inflammatory infiltrate, which were identified by the lack of fluorescence and a darkened appearance.

Inflammatory cell count (neutrophils)

The neutrophil count was subsequently performed for the same representative sections using light microscopy and was based on their morphological characteristics (i.e. darkly stained cells with multilobed, horseshoe-shaped nuclei). The neutrophils were counted in the middle region of the lesion, adjacent to the apical foramen, in an area of approximately 0.08 mm², according to De Rossi *et al.* (2008) and Da Silva *et al.* (2012). The results are expressed as the number of cells.

Tartrate-resistant acid phosphatase (TRAP) activity histochemistry

TRAP activity was used for osteoclast staining and counting as described by Da Silva *et al.* (2012). The results are expressed as cell number, according to Da Silva *et al.* (2012).

Brown and Brenn modified staining

Brown & Brenn (1931) staining was used to assess the presence or absence of bacteria and their location in the crown of the tooth, root canal system and periapical tissues (cementum, periodontal ligament and alveolar bone; Chen *et al.* 1999). Scores from 0 to 5 were assigned for this assessment (De Rossi *et al.* 2008, Da Silva *et al.* 2012) using the following system: 0, the absence of bacteria; 1, the presence of bacteria in the tooth's crown; 2, the presence of bacteria in the cervical third of the root canal; 3, the presence of bacteria in the middle third of the root canal; 4, the presence of bacteria in the apical third of the root canal; and 5, the presence of bacteria in the periapical lesion.

Immunohistochemistry

The reactions were performed using the avidin–biotin–peroxidase complex method (indirect method),

as described by Da Silva *et al.* (2012). The primary antibodies that were used were anti-RANK (polyclonal rabbit antibody H300 sc:9072, diluted 1:700; Santa Cruz Biotechnology Inc., Dallas, TX, USA), anti-RANKL (polyclonal goat antibody n-19 sc:7628; Santa Cruz Biotechnology Inc.; diluted 1:400) and anti-OPG (polyclonal goat antibody n-20 sc:8468; Santa Cruz Biotechnology Inc.; diluted 1:700). The slides were incubated with biotinylated secondary antibody (goat anti-rabbit IgG-B sc-2040 and rabbit anti-goat IgG-B sc-2774; Santa Cruz Biotechnology Inc., diluted 1:200). The identification of osteoclastogenesis markers was performed using an Axio Imager.M1 microscope under conventional light. The results are expressed qualitatively, considering the presence/absence and location of markers, as described by Da Silva *et al.* (2012).

Statistical analysis

The comparison of the areas of the periapical lesions, the number of osteoclasts and the number of inflammatory cells between periods within the same group of animals (WT and MyD88 KO) was performed using the nonparametric Kruskal–Wallis test and Dunn's post-test. The comparisons for samples following the same period of time between different groups of animals (WT and KO MyD88) were performed using the nonparametric Mann–Whitney test. The data were analysed using the Statistical Package for the Social Sciences SPSS software (version 17.0; SPSS Inc, Chicago, IL, USA), at a 5% significance level.

Results

Descriptive microscopic analysis of the characteristics of the root canal and both the apical and periapical regions

WT animals exhibited total necrosis of the pulp tissue 7 days following periapical lesion induction. The periodontal ligament was slightly enlarged, with the occasional presence of inflammatory cells, which were predominantly mononuclear. The cementum surface was regular, without resorption areas. The alveolar bone was normal, with osteoblasts on their surface. The median lesion size in this period was $60\,842.5\ \mu\text{m}^2$ (Fig. 1a,b). At the 21-day time-point, the pulp tissue was completely necrotic, and the root cementum exhibited surface irregularities. The periodontal ligament was enlarged, with extensive oedema

and areas of fibrillar dissociation. Predominantly mononuclear inflammatory cells were scattered throughout the region. The alveolar bone was observed to be bare and to exhibit areas of resorption. The median lesion size at this time was $74\,368.0\ \mu\text{m}^2$ (Fig. 1e, f). The radicular pulp exhibited total necrosis at day 42. The periodontal ligament was severely enlarged, exhibiting dense inflammatory infiltrate, predominantly mononuclear, diffusely throughout the region. The cementum and alveolar bone exhibited extensive resorption areas. The median lesion size at this time was $258\,088.0\ \mu\text{m}^2$ (Fig. 1i,j).

With respect to MyD88 KO animals, the specimens also exhibited total necrosis of the pulp tissue at day 7 as determined by the descriptive analyses. The periodontal ligament was moderately enlarged, exhibiting mixed and diffuse inflammatory infiltrate, with the considerable presence of neutrophils. The surface cementum was regular, whereas the alveolar bone exhibited resorption areas and no osteoblasts on its surface. Moreover, the periodontal ligament exhibited areas of oedema onset and fibrillar dissociation. The median lesion size at this time was $123\,803.0\ \mu\text{m}^2$ (Fig. 1c,d). At day 21, the pulp tissue was completely necrotic. The cementum exhibited early resorption areas, making its surface slightly irregular. The periodontal ligament was enlarged, with areas of oedema and the dissociation of collagen fibres. There was mixed inflammatory infiltrate with mononuclear and polymorphonuclear cells spread throughout the periapical region, with the considerable presence of neutrophils. The alveolar bone was observed to be bare, with areas of resorption. The median lesion size at this time was $153\,306.0\ \mu\text{m}^2$ (Fig. 1g,h). At 42 days, the radicular pulp exhibited total necrosis. The periodontal ligament was severely enlarged, with fibrillar dissociation and oedema. A dense mixed inflammatory cell infiltrate was observed diffusely across the region, with the presence of abundant neutrophils. The alveolar bone far from the root apex did not have osteoblasts on its surface. The root cementum was irregular due to resorption areas, and there was intense resorption activity in the alveolar bone, with a strong presence of clastic cells. The median lesion size at this time was $467\,777.0\ \mu\text{m}^2$ (Fig. 1k,l).

Briefly, the descriptive microscopic analysis revealed a more intense inflammatory infiltrate, with the abundant presence of mononuclear and polymorphonuclear cells and extensive tissue destruction, in the MyD88 KO group compared with the WT mice, which predominantly showed

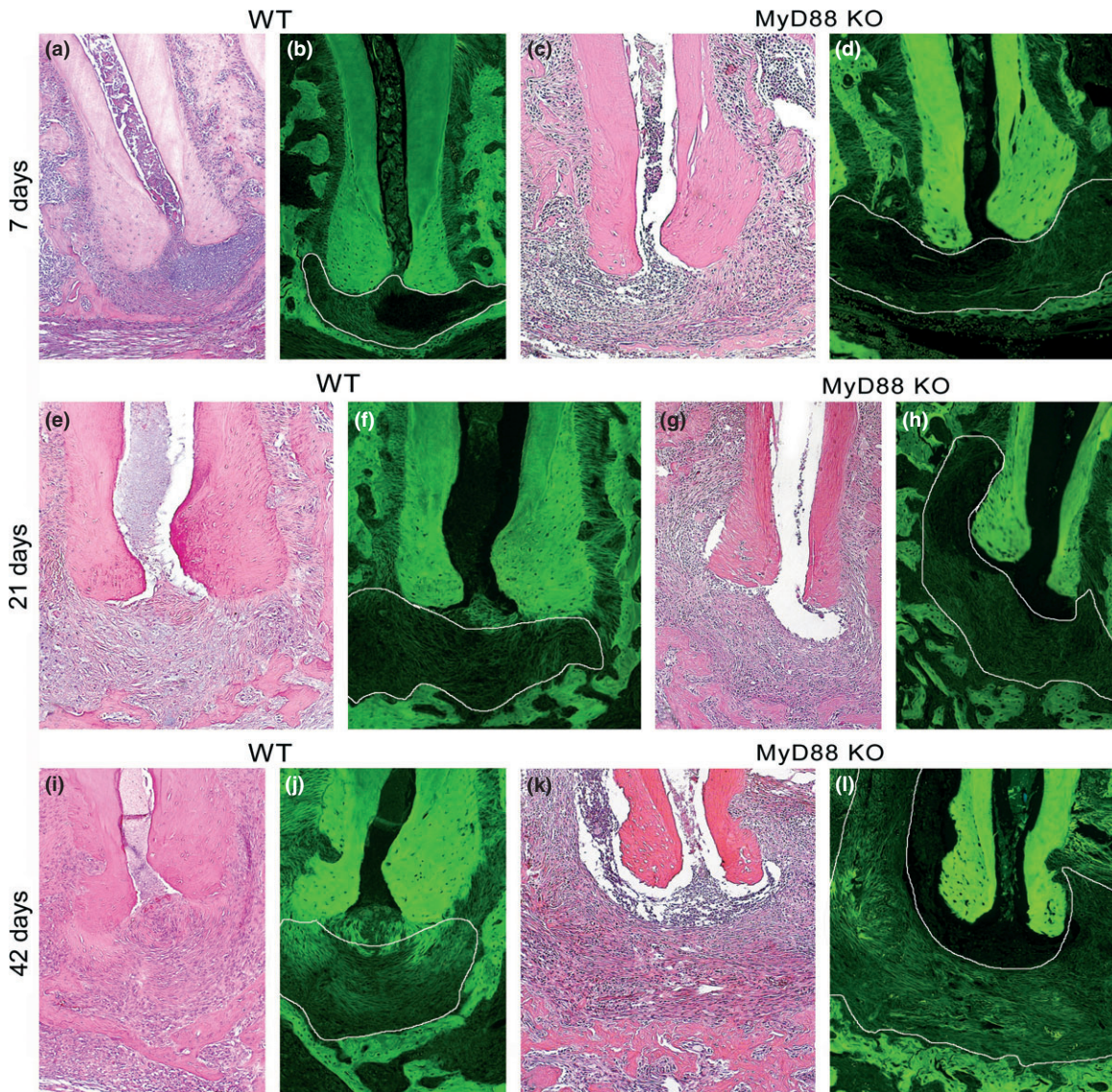


Figure 1 Photomicrographs of representative HE-stained microscopic sections of WT and MyD88 KO animals at 7-, 21- and 42-day experimental periods. In a, c, e, g, i and k, the sections were observed under conventional light microscopy for a descriptive analysis of the root canal system and apical and periapical regions and for measurement of neutrophil counts. In b, d, f, h, j and l, the images were obtained by the fluorescence technique for measuring the size of periapical lesions (10 \times).

mononuclear cells (Fig. 2e,f). Figure 2 presents microscopic events observed during the descriptive analysis of the root canal system and apical and periapical regions.

Fluorescence microscopy morphometrics

A significant difference between the time-points was observed in the WT mice group, and Dunn's post-test indicated that the lesions were significantly larger at

the 42-day time-point than at the 7- ($P < 0.001$) and 21-day ($P = 0.001$) time-points. With respect to the My88 KO group, measures were also observed to be significantly higher at the 42-day time-point than at the 7- ($P = 0.001$) and 21-day ($P = 0.005$) time-points.

The comparison of the 7-, 21- and 42-day time-points between the MyD88 KO (Fig. 1d, h and l) and WT (Fig. 1b, f and j) groups revealed a significant difference in the experimental 7- ($P = 0.001$) and 21-day ($P = 0.05$) time-point, with significantly

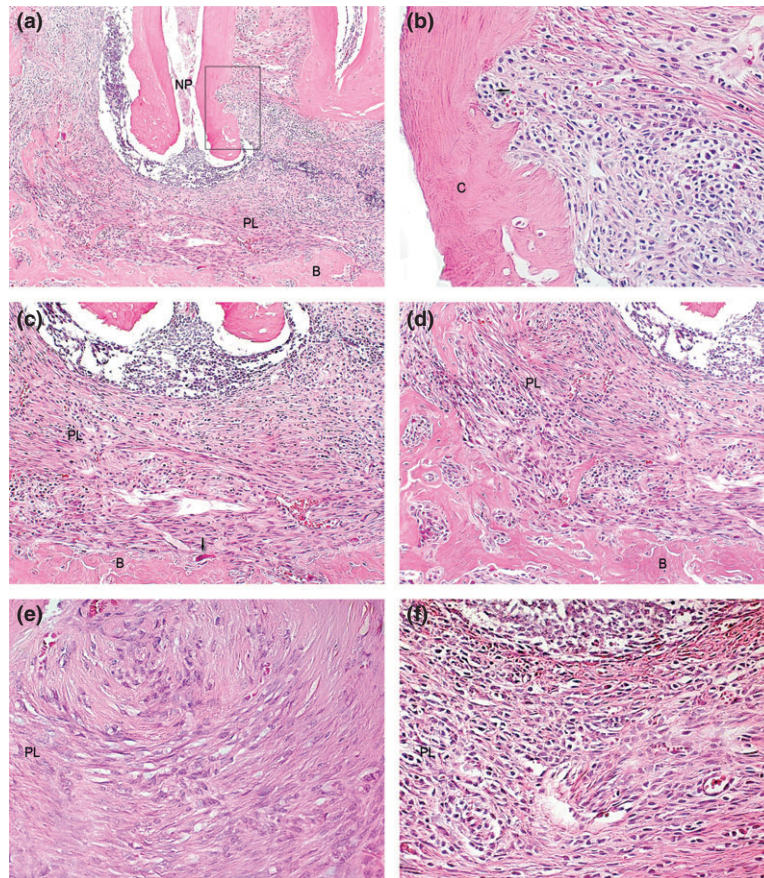


Figure 2 Photomicrographs obtained under conventional light microscopy representative of the microscopic events observed during the descriptive analysis of the root canal system and apical and periapical regions after experimental induction of periapical lesions in the WT and MyD88 KO animals, at the different experimental periods: (a) apical and periapical regions. Necrotic pulp tissue (NP), severely increased width of the periodontal ligament (PL) space and bone alveolar (B) with resorption areas (MyD88 KO – 42 days; 10 \times). (b) Detail of image A (square) showing the cemental surface (C) with resorption areas (arrow), fibrillar dissociation and inflammatory cells (MyD88 KO – 42 days; 40 \times). (c) Detail of image A revealing a severely increased width of the periodontal ligament (PL) space, with areas of oedema and fibrillar dissociation, mixed and diffuse inflammatory infiltrate, and large number of neutrophils. The alveolar bone (B) appears denuded and exhibits osteoclasts (arrow) on its surface (MyD88 KO – 42 days; 40 \times). (d) Detail of image A showing increased width of the periodontal ligament (PL) space and alveolar bone (b) distant from the root apex and severely resorbed (MyD88 KO – 42 days; 40 \times). (e) Periodontal ligament (PL) with dense, diffuse, predominantly mononuclear infiltrate inflammatory, characteristic of WT group (WT – 42 days; 40 \times). (f) Periodontal ligament (PL) with dense, diffuse, mixed infiltrate inflammatory, with large number of neutrophils, characteristic of MyD88 KO group (MyD88 KO – 42 days; 40 \times).

higher values for the MyD88 KO group. With respect to the 42-day time-point, there was a numerical trend towards the same behaviour, but no statistically significant difference was observed ($P = 0.09$).

Table 1 outlines the median, minimum and maximum values of periapical lesion area based on fluorescence microscopy analysis and the statistical analysis of the results. The results are given for all of the experimental periods (7, 21 and 42 days) and for the different groups (WT and MyD88 KO).

Inflammatory cell count (neutrophils)

A significant difference was observed in the WT mice between the periods of evaluation ($P = 0.01$). The number of neutrophils that were observed at the 21-day time-point was significantly higher than at the 7- ($P < 0.01$) and 42-day ($P = 0.03$) time-points. With respect to the MyD88 KO group, the values observed at the 42-day time-point were significantly higher than for the 21-day ($P = 0.01$) time-point,

Table 1 The comparison between the fluorescence microscopy-based periapical lesion area measurements at different experimental time-points for MyD88 KO and WT animals and between the different groups of animals following the same periods of evaluation

	7 days M (Mn–Mx)	21 days M (Mn–Mx)	42 days M (Mn–Mx)	<i>P</i> *
WT	60 842.5 (26 446.0–106 925.0)	74 368.0 (23 738.0–278 760.0)	258 088.0(87 696.0–765 935.0)	<0.001
MYD88 KO	123 803.0 (92 083.0–175 784.0)	153,306.0 (85 444.0–242 377.0)	467 777.0 (101 560.0–759 868.0)	0.002
<i>P</i> **	0.001	0.05	0.09	

M: median; Mn: minimum; Mx: maximum; *P**: Kruskal–Wallis test; *P*** : Mann–Whitney test.

whereas no significant difference was observed between the other periods.

The comparison of the 7-, 21- and 42-day time-points between the MyD88 KO and WT groups revealed a significant difference at the 7- ($P = 0.01$), 21- ($P = 0.004$) and 42-day ($P < 0.001$) time-points, with significantly higher values for the MyD88 KO group.

Table 2 outlines the median, minimum and maximum values of the neutrophil counts that were found in the middle region of the lesion, adjacent to the apical foramen and the statistical analysis of the results. The results are given for each of the experimental periods (7, 21 and 42 days) and for the different groups (WT and MyD88 KO).

Histoenzymology of tartrate-resistant acid phosphatase (TRAP) activity

For both of the groups, (i.e. WT and MyD88 KO), no significant difference in osteoclast count was observed between the 7-, 21- and 42-day time-points ($P = 0.226$ and 0.457 , respectively). The comparison of the 7-, 21- and 42-day time-points between the WT and MyD88 KO groups also revealed no significant difference for the experimental 7-day ($P = 0.884$), 21- ($P = 0.506$) or 42-day ($P = 0.211$) time-points. TRAP-staining-positive cells surrounding the periapical lesions of the WT and MyD88 KO groups are illustrated in Fig. 3.

Table 3 outlines the medians, minimum and maximum values of the osteoclast count in the resorption lacunae and in direct contact with the alveolar bone surrounding the periapical lesions. The statistical results are given for the experimental periods (7, 21 and 42 days) and for the different groups (WT and MyD88 KO).

Modified Brown and Brenn staining

With respect to the assessment of bacterial presence and location in the root canal system and periapical tissues, specimens from the group of WT animals were rated with a score of 4 at days 7, 21 and 42. The presence of a large amount of bacteria was noted in the tooth crown and the cervical third of the root canal, including the dentinal tubules and the interradicular region. The amount of bacteria progressively decreased towards the apical region, with small number of bacteria in the middle and apical thirds and no bacteria detected in the periapical lesions. Conversely, in the MyD88 KO group, microbial infection was more strongly spread throughout the root canal system, including the periapical region and the lesion; this group was rated with a score of 5. Bacteria were found abundantly in the tooth crown and the cervical and middle thirds of the root canal, with deep penetration in the dentinal tubules. The specimens exhibited bacteria in the apical third, the foramen exit, the cement lacunae and the periapical lesion (Fig. 4).

Table 2 The comparison between the neutrophil counts at the different experimental periods in MyD88 KO and WT animals and between the different groups of animals following the same evaluation periods

	7 days M (Mn–Mx)	21 days M (Mn–Mx)	42 days M (Mn–Mx)	<i>P</i> *
WT	13.0 (10.5–18.0)	25.0 (16.0–41.0)	16.0 (12.5–26.0)	0.01
MYD88 KO	109.0 (69.0–158.5)	85.0 (46.5–112.5)	158.0 (70.5–246.0)	0.02
<i>P</i> **	0.01	0.004	<0.001	

M: median; Mn: minimum; Mx: maximum; *P**: Kruskal–Wallis test; *P*** : Mann–Whitney test.

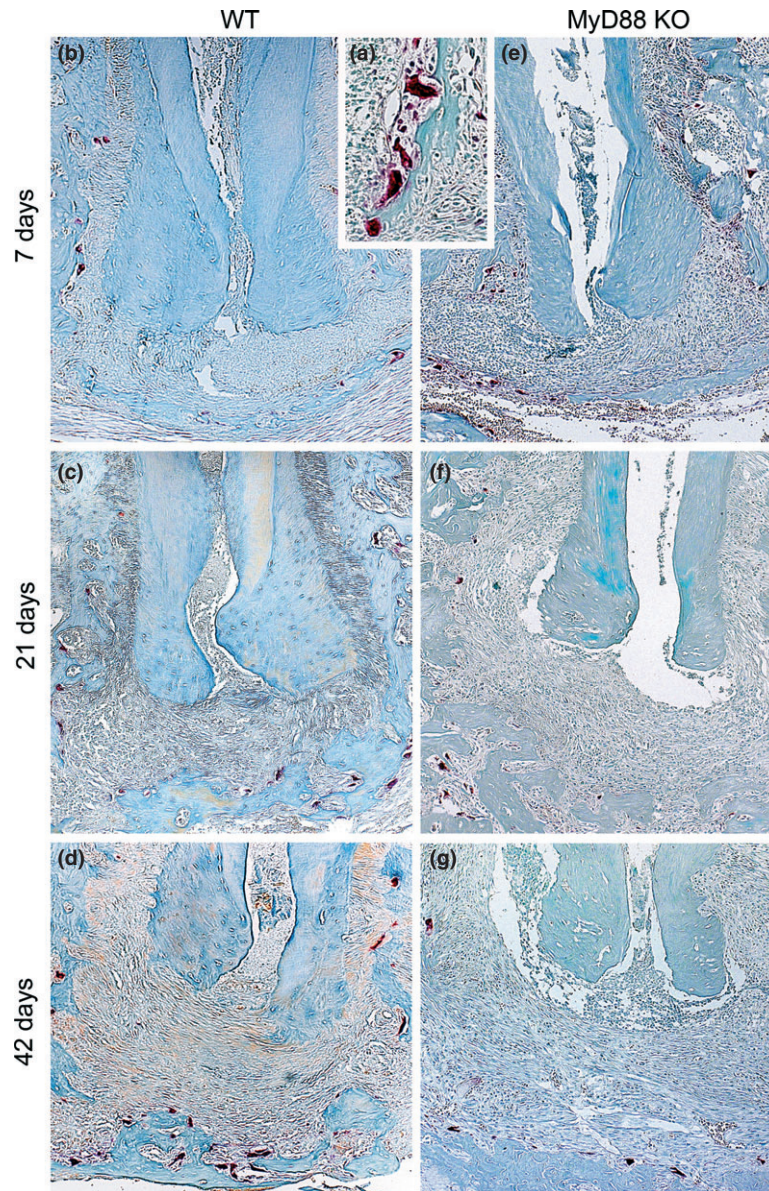


Figure 3 Photomicrographs of representative microscopic sections of WT animals (a, b, c and d) and MyD88 KO animals (e, f and g) at 7-, 21- and 42-day experimental periods, stained with the tartrate-resistant acid phosphatase (TRAP) histoenzymology technique for identification and counting of osteoclasts (10x). Image A shows osteoclastic cells present in the resorption lacunae in direct contact with the alveolar bone surrounding the periapical lesion of WT animal (40x).

Immunohistochemistry

RANK-positive staining was noted in specimens from both of the groups, generally in the apical foramen region. RANKL staining was noted in specimens in both the MyD88 KO and WT groups at 7, 21 and 42 days, primarily in the apical foramen region and within the periapical lesion. OPG staining was noted

in specimens from animals of the WT and MyD88 KO groups, especially within the lesion, at all of the experimental periods. Staining was also noted in the specimens from the WT group at the ends of the periapical lesion. Photomicrographs that are representative of RANK, RANKL and OPG staining are shown in Fig. 5, indicating their locations.

Table 3 The comparison of the osteoclast counts following different experimental periods in MyD88 KO and WT animals and between the different groups of animals following the same periods of evaluation

	7 days M (Mn-Mx)	21 days M (Mn-Mx)	42 days M (Mn-Mx)	<i>P</i> *
WT	7.5 (4.0–27.5)	8.0 (1.5–34.5)	14.0 (3.5–35.5)	0.226
MYD88 KO	10.25 (3.0–15.5)	10.25 (6.5–16.0)	12.0 (8.0–17.0)	0.457
<i>P</i> **	0.884	0.506	0.211	

M: median; Mn: minimum; Mx: maximum; *P**: Kruskal–Wallis test; *P****: Mann–Whitney test.

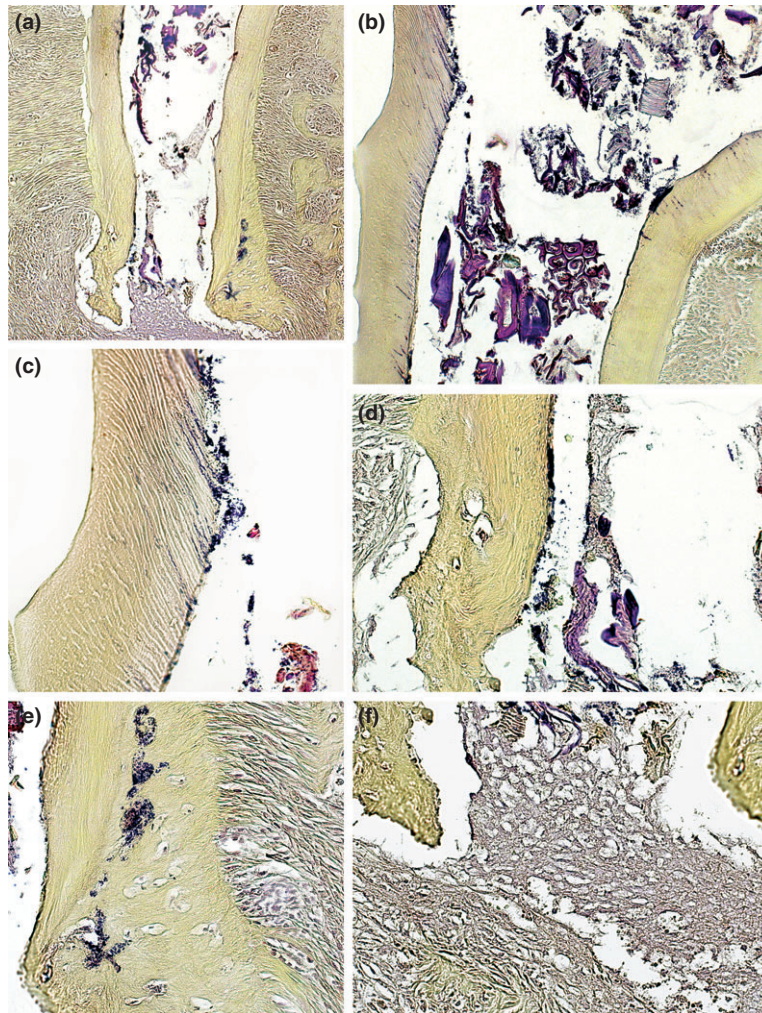


Figure 4 Photomicrographs of representative microscopic sections of MyD88 KO animals stained with the modified Brown and Brenn technique showing the presence and location of bacteria in the root canal system and periapical tissues: (a) Panoramic photomicrograph revealing intense bacterial contamination in all tooth extension (10 \times). (b) Coronal root canal third with a large number of microorganisms (40 \times). (c) Detail of image B in which dentinal tubules with intense presence of bacteria can be seen. (d) Detail of image A in which microorganisms can be seen in the apical third and resorption craters. (e) Detail of image A showing a large number of bacteria in the cemental lacunae. (f) Detail of image A showing microorganisms in the periapical lesion.

Discussion

The results found in the current study evidenced that MyD88 KO mice developed more extensive periapical

lesions than WT animals, most likely due to the damage to the immune system caused by the lack of the adapter molecule MyD88, which participates in TLR

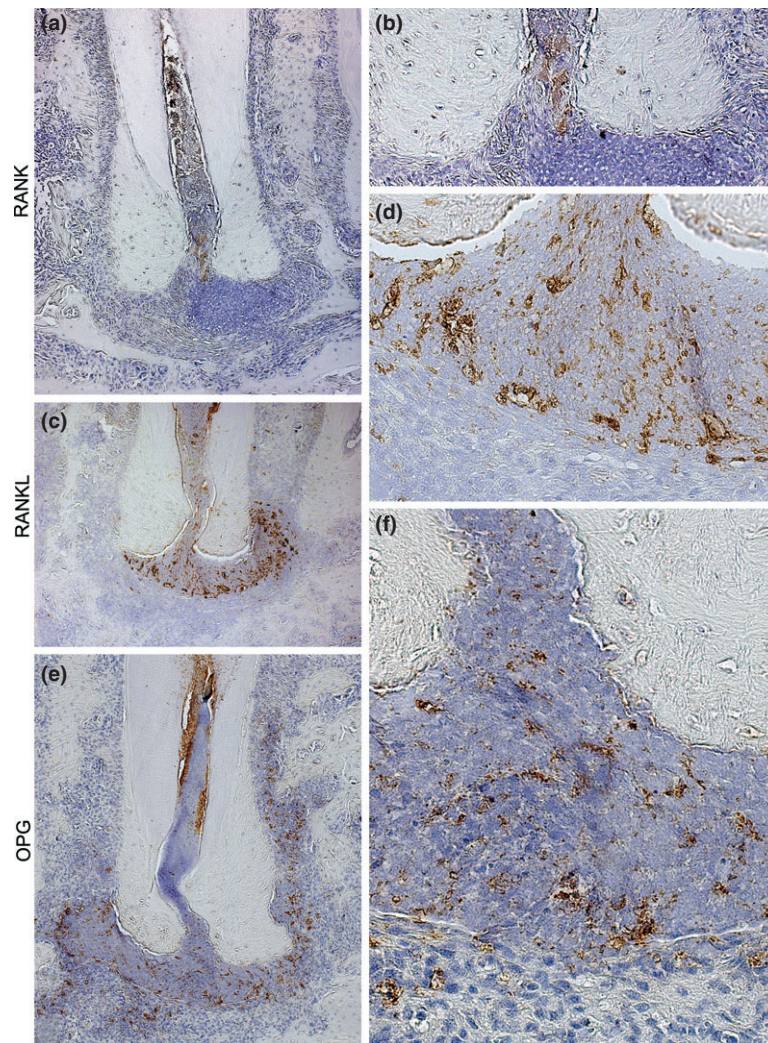


Figure 5 Photomicrographs representative of microscopic sections of WT and MyD88 KO animals subjected to the immunohistochemical technique for detection of the osteoclastogenesis markers RANK, RANKL and OPG, at the different experimental periods, indicating their locations (a, c, e - 10 \times ; b, d, f - 40 \times).

signalling. A progressive increase in periapical lesion size was noted from the beginning of the experiment to the end, and MyD88 KO animals developed markedly larger lesions by the 7- and 21-day time-points. Although there was no statistically significant difference on the 42-day time-point, periapical lesions of the MyD88 KO animals were larger and there was a numerical trend towards the same behaviour observed on the previous time-points. This observation was correlated with differences in the characteristics of inflammatory infiltrate, which was further exacerbated and showed a considerable presence of neutrophils and mononuclear cells in MyD88 KO animals, with deficient control of its chronification.

In the current study, the quantitative analysis of neutrophil number confirmed the qualitative description and revealed a significantly higher number of these cells in the MyD88 KO group than in WT animals at all of the time-points. Neutrophils have a very brief lifespan and act within the inflammatory infiltrate for approximately 3 days (Reinke & Sorg 2012), indicating that the bacterial aggressor stimulus was more intense and persistent in the MyD88 KO group, stimulating neutrophil migration until the final time-point of the experiment. Moreover, it is possible that molecular events and the mechanisms that are involved in the control of neutrophil influx to inflammatory sites are mediated by MyD88.

The lack of studies evaluating the effect of the molecule MyD88 on the development of periapical lesions precludes a direct comparison with the present results. However, the current study is consistent with previous results, which demonstrated that the MyD88 signalling pathway is essential for infection control and for the adequate and efficient organization of the inflammatory and immune response (LaRosa *et al.* 2008, Koh *et al.* 2010, Loures *et al.* 2011).

In this context, the noted difference in bacterial presence and location between groups, as shown by Brown and Brenn staining, stands out. Bacteria were more severely disseminated throughout the root canal system in the MyD88 KO group, being abundantly found in the cervical, middle and apical thirds, including the periapical lesion, indicating a loss of host resistance and infection fighting ability in MyD88 KO mice, which is consistent with previous studies.

MyD88 is used by all of the TLRs, except TLR3, and transduces signals that culminate in NF- κ B activation, the induction of pro-inflammatory mediators, including TNF- α and IL-6, and the production of IFN types I, α and β (Siednienko *et al.* 2011). Furthermore, MyD88 activates IL-1 (IL-1R, IL-18R and IL-33R) receptors, and consequently, the intracellular signalling and cytokine production that are induced by these receptors are also down-regulated in the absence of this adapter molecule (Kawai & Akira 2011, Loures *et al.* 2011). In this field, it was shown that MyD88 expression in dental follicle cells leads to monocyte chemoattractant protein-1 (MCP-1) and RANKL up-regulation, which is needed for osteoclastogenesis (Liu *et al.* 2010a). Thus, the genetic deletion of MyD88 in the current study promoted the silencing of many key signalling pathways, which most likely exacerbated the inflammatory process, increased the area of the periapical lesions and resulted in the dysfunctional activation and organization of the immune response. These findings are in agreement with Graves *et al.* (2011), who reported that the inhibition of an immune response component in endodontic lesions causes a reduction in resistance to bacterial infection and the formation of more extensive osteolytic lesions.

Therefore, MyD88 molecule plays a key role during inflammatory and immune responses that are triggered to fight infections in the root canal system and the periapical tissue during the genesis and the development of periapical lesions, indicating a protective function.

In agreement with the literature (De Rossi *et al.* 2008, Liu *et al.* 2010b, Xiong *et al.* 2010, Silva *et al.* 2011, Da Silva *et al.* 2012), osteoclasts were observed to be associated with the resorption areas in the periapical regions of WT and MyD88 KO mouse teeth in the current study. However, differences in the number of these cells were not observed between the groups following any of the experimental periods. This result suggests that the increased tissue destruction that was observed in specimens in the MyD88 KO group may have also been caused by other immunoinflammatory mechanisms in addition to those inducing osteoclast differentiation and activation. These mechanisms include the expression of pro-inflammatory cytokines, which may have been increased by the presence of more aggressive products, by-products and other virulent factors in the endodontic infections of MyD88 KO animals.

Based on immunohistochemical analysis, similar levels of RANK, RANKL and OPG staining were observed in WT and MyD88 KO animals at the 7-, 21- and 42-day time-points. Therefore, the involvement of these osteoclastogenesis mediators in periapical lesion development is confirmed, as previously described (Vernal *et al.* 2006, Menezes *et al.* 2008, Moraes *et al.* 2011, Da Silva *et al.* 2012).

Importantly, this is the first study to evaluate the effects of the adapter molecule MyD88 on endodontic infections and the development of periapical lesions, precluding direct comparison of the current results with those of previous studies. Further studies are required to elucidate the functions that are performed by this molecule and the mechanisms that are triggered upon its genetic silencing. Such mechanisms include compensation, stimulation and inhibition of immunoinflammatory events and bone resorption following the recognition of microorganisms and periapical lesion onset.

Conclusion

MyD88 KO animals developed more extensive periapical lesions, with a severe inflammatory infiltrate and significantly greater numbers of neutrophils than WT animals. Therefore, the null hypothesis was rejected.

Acknowledgements

We thank Marco Antonio dos Santos and Nilza Letícia Magalhães, laboratory technicians of Department of Pediatric Dentistry, School of Dentistry of

Ribeirão Preto, University of São Paulo, Ribeirão Preto, SP, Brazil, for the histotechnical processing carried out in this work. We thank the financial support received by grant #2012/25020-1, São Paulo Research Foundation (FAPESP).

References

- Bar-Shavit Z (2008) Taking a toll on the bones: regulation of bone metabolism by innate immune regulators. *Autoimmunity* **41**, 195–203.
- Brown JH, Brenn L (1931) A method for the differential staining of Gram-positive and Gram-negative bacteria in tissue sections. *Bulletin of the Johns Hopkins Hospital* **48**, 69–73.
- Chen CP, Hertzberg M, Jiang Y, Graves DT (1999) Interleukin-1 and tumor necrosis factor receptor signaling is not required for bacteria-induced osteoclastogenesis and bone loss but is essential for protecting the host from a mixed anaerobic infection. *American Journal of Pathology* **155**, 2145–52.
- Da Silva RAB, Ferreira PDF, De Rossi A, Nelson-Filho P, Silva LAB (2012) Toll-like receptor2 knockout mice showed increased periapical lesion size and osteoclast number. *Journal of Endodontics* **38**, 803–13.
- De Rossi A, Rocha LB, Rossi MA (2007) Application of fluorescence microscopy on hematoxylin and eosin-stained sections of healthy and diseased teeth and supporting structures. *Journal of Oral Pathology & Medicine* **36**, 377–81.
- De Rossi A, Rocha LB, Rossi MA (2008) Interferon-gamma, interleukin-10, Intercellular adhesion molecule-1, and chemokine receptor 5, but not interleukin-4, attenuate the development of periapical lesions. *Journal of Endodontics* **34**, 31–8.
- Gomes MT, Campos PC, de Almeida LA *et al.* (2012) The role of innate immune signals in immunity to *Brucella abortus*. *Frontiers in Cellular and Infection Microbiology* **2**, 1–9.
- Graves DT, Oates T, Garlet GP (2011) Review of osteoimmunology and the host response in endodontic and periodontal lesions. *Journal of Oral Microbiology* **17**, 1–15.
- Hanke ML, Angle A, Kielian T (2012) MyD88-dependent signaling influences fibrosis and alternative macrophage activation during *Staphylococcus aureus* biofilm infection. *PLoS ONE* **7**, e42476.
- Hedayat M, Takeda K, Rezaei N (2012) Prophylactic and therapeutic implications of toll-like receptor ligands. *Medical Care Research and Review* **32**, 294–325.
- Hirao K, Yumoto H, Takahashi K, Mukai K, Nakanishi T, Matsuo T (2009) Roles of TLR2, TLR4, NOD2, and NOD1 in pulp fibroblasts. *Journal of Dental Research* **88**, 762–7.
- Hughes MA, Green CS, Lowchjy L *et al.* (2005) MyD88-dependent signaling contributes to protection following *Bacillus anthracis* spore challenge of mice: implications for Toll-like receptor signaling. *Infection and Immunity* **73**, 7535–40.
- Ishibashi D, Atarashi R, Nishida N (2012) Protective role of MyD88-independent innate immune responses against prion infection. *Prion* **6**, 443–6.
- Kawai T, Akira S (2009) The roles of TLRs, RLRs and NLRs in pathogen recognition. *International Immunology* **21**, 317–37.
- Kawai T, Akira S (2011) Toll-like receptors and their crosstalk with other innate receptors in infection and immunity. *Immunity* **34**, 637–50.
- Koh YS, Koo JE, Biswas A, Kobayashi KS (2010) MyD88-dependent signaling contributes to host defense against ehrlichial infection. *PLoS ONE* **5**, e11758.
- LaRosa DF, Stumhofer JS, Gelman AE *et al.* (2008) T cell expression of MyD88 is required for resistance to *Toxoplasma gondii*. *Proceedings of the National Academy of Sciences of the United States of America* **105**, 3855–60.
- Liu D, Yao S, Wise GE (2010a) MyD88 expression in the rat dental follicle: implications for osteoclastogenesis and tooth eruption. *European Journal of Oral Sciences* **118**, 333–41.
- Liu S, Cheng Y, Xu W, Bian Z (2010b) Protective effects of follicle-stimulating hormone inhibitor on alveolar bone loss resulting from experimental periapical lesions in ovariectomized rats. *Journal of Endodontics* **36**, 658–63.
- Loures FV, Pina A, Felonato M, Feriotti C, de Araújo EF, Calich VL (2011) MyD88 signaling is required for efficient innate and adaptive immune responses to *Paracoccidioides brasiliensis* infection. *Infection and Immunity* **79**, 2470–80.
- Menezes R, Garlet TP, Letra A *et al.* (2008) Differential patterns of receptor activator of nuclear factor kappa B ligand/osteoprotegerin expression in human periapical granulomas: possible association with progressive or stable nature of the lesions. *Journal of Endodontics* **34**, 932–8.
- Moraes M, Lucena HF, Azevedo PR, Queiroz LM, Costa AD (2011) Comparative immunohistochemical expression of RANK, RANKL and OPG in radicular and dentigerous cysts. *Archives of Oral Biology* **56**, 1256–63.
- Reinke JM, Sorg H (2012) Wound repair and regeneration. *European Surgical Research* **49**, 35–43.
- Siednienko J, Gajanayake T, Fitzgerald KA, Moynagh P, Miggin SM (2011) Absence of MyD88 results in enhanced TLR3-dependent phosphorylation of IRF3 and increased IFN- β and RANTES production. *The Journal of Immunology* **186**, 2514–22.
- Silva MJ, Sousa LM, Lara VP *et al.* (2011) The role of iNOS and PHOX in periapical bone resorption. *Journal of Dental Research* **90**, 495–500.
- Vernal R, Dezerega A, Dutzan N *et al.* (2006) RANKL in human periapical granuloma: possible involvement in periapical bone destruction. *Oral Disease* **12**, 283–9.
- Xiong H, Wei L, Hu Y, Zhang C, Peng B (2010) Effect of alendronate on alveolar bone resorption and angiogenesis in rats with experimental periapical lesions. *International Endodontic Journal* **43**, 485–91.